Negative Poisson Ratio of Crystalline Cellulose in Kraft Cooked Norway Spruce

Marko Peura,[†] Ingo Grotkopp,[‡] Henrik Lemke,[‡] Anne Vikkula,[§] Janne Laine,[§] Martin Müller,[‡] and Ritva Serimaa*,[†]

Department of Physical Sciences, Division of X-ray Physics, P.O. Box 64, FI-00014 University of Helsinki, Finland, Institut für Experimentelle und Angewandte Physik der Christian-Albrechts-Universität zu Kiel, Leibnizstraβe 19, D-24098 Kiel, Germany, and Laboratory of Forest Products Chemistry, P.O. Box 6300, FI-02015 Helsinki University of Technology, Finland

Received September 27, 2005; Revised Manuscript Received December 21, 2005

The tensile properties of kraft cooked Norway spruce were studied by tensile testing with in situ X-ray diffraction (XRD). Samples were of earlywood, cooked for varying times. The total lignin content of the samples was between 21.7% and 9.3%. Tensile tests with XRD were performed on wet samples, without XRD on dry samples. The tensile strength, the modulus of elasticity (MOE), and the elongation at fracture/yield were determined. X-ray diffraction was used to determine the microfibril angle (MFA) and the deformation of crystalline cellulose by monitoring the reflections *200* and *004*. The (X-ray) Poisson ratio of crystalline cellulose was calculated, both before and after the yield point. The tensile strength and the MOE of the wet samples were significantly lower than in the dry samples. The tensile properties of dry samples were similar to dry earlywood samples of untreated Norway spruce. The MFA only showed notable changes due to strain when it was initially large, when a diminishing effect was observed. The Poisson ratio of crystalline cellulose was negative. The average values ranged between −0.26 and −1.17 before the yield point and between −0.86 and −1.05 after the yield point.

Introduction

Wood is a cellular solid with a complex, varying structure. In a mechanical sense, the structure−property relationships of wood in a scale of several annual rings or entire stems are nevertheless fairly well-known. There is a wealth of information concerning the mechanical properties of different wood species on this scale, see e.g. the book by Wagenführ and Scheiber.[1] Developments in instrumentation have increased the possibilities of various studies on the mechanical properties of small scale samples. Samples containing single or few cells from selected positions within single annual rings can be studied with respect to macroscopic and ultrastructural parameters simultaneously. For instance, the strength of the sample and the orientation of crystalline cellulose in the cell walls have both been studied at the same time.[2−5] Such diverse combinative studies have revealed a complex interplay between the chemical constituents of wood, which is yet only partially understood.

Studies on the mechanical properties of small wood samples or single cells are currently performed with a variety of different methods, nearly all including some kind of in situ deformation. Environmental scanning electron microscope (ESEM)[6,7] or light microscopy[8,9] have been used to characterize the fracture processes and the tensile properties of the entire samples. Fourier transform infrared (FTIR)[10,11] and Raman[12] spectroscopy have been used to probe the effect of strain on the macromolecular components of wood.

The tensile properties of wood in the direction parallel to the longitudinal cell axis are largely dominated by the tensile properties of cellulose. In crystalline cellulose, the cellobiose units are bonded with strong covalent bonds and form chains along the crystallographic *c* axis, see Figure 1. The neighboring chains are hydrogen-bonded and form planar sheets along the axis *b*. The sheets are stacked along the axis *a*, held together only by weak van der Waals-type of interactions.[13−16]

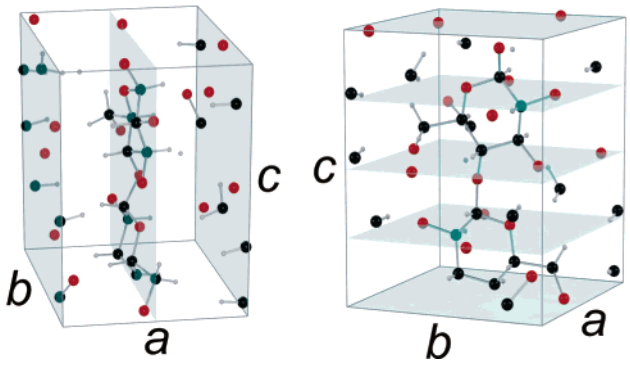

Figure 1. Schematic drawing of the unit cell of crystalline cellulose I_β. The unit cell is based on a recent structural study[16] and was drawn with the programs BAM PowderCell 2.4 and POV-Ray 3.6. The reflection planes *200* and *004* are shown on the left and right, respectively.

The tensile properties of crystalline cellulose are also dominant to the tensile properties of single wood cells, at least if the cellulose microfibrils are oriented nearly parallel to the cell axis. The studies of wood on a macromolecular level have revealed that in the direction perpendicular to the cellulose chains the other, amorphous constituents of wood (mainly hemicelluloses and lignin) have a notable effect on the mechanical properties of wood material.[17] Therefore, to gain more knowledge about the tensile properties of crystalline cellulose in wood, it is of interest to examine wood material modified in such a way that the amorphous matrix is selectively gradually

* Corresponding author. Phone: +358-9-191 50632. Fax: +358-9-191 50639. E-mail: Ritva.Serimaa@helsinki.fi.
[†] University of Helsinki.
[‡] Universität zu Kiel.
[§] Helsinki University of Technology.

10.1021/bm050722o CCC: $33.50
Published on Web 04/05/2006

Table 1. Chemical Composition of the Samples[a]

t_C [min]	Y [%]	k	AR [%]	XYL [%]	MAN [%]	GLU [%]	TCH [%]	GLI [%]	DLI [%]	TLI [%]	EX [%]
120	60.6	65.1	0.74	5.78 ± 0.10	4.51 ± 0.08	67.7 ± 1.2	78.7 ± 1.2	20.69	1.00	21.69	0.24 ± 0.01
150	55.0	64.0	0.72	6.36 ± 0.09	4.84 ± 0.07	76.2 ± 1.1	88.1 ± 1.1	16.16	0.73	16.89	0.25 ± 0.02
180	50.6	57.6	0.77	6.39 ± 0.11	5.44 ± 0.10	80.2 ± 1.4	92.8 ± 1.4	11.98	0.59	12.57	0.24 ± 0.02
210	49.9	41.5	0.59	6.95 ± 0.12	4.90 ± 0.09	84.2 ± 1.5	96.5 ± 1.5	10.05	0.49	10.54	0.35 ± 0.05
240	48.2	38.3	0.52	6.60 ± 0.12	5.15 ± 0.09	84.2 ± 1.5	96.5 ± 1.5	8.82	0.45	9.27	0.24 ± 0.04

[a] t_C denotes the cooking time, Y is the yield of the cook, and κ is the kappa number. AR denotes the mass fraction of arabinose, XYL xylose, MAN mannose. GLU is the mass fraction of glucose and galactose combined, and TCH is the total amount of carbohydrates. GLI denotes the mass fraction of gravimetric lignin, DLI denotes the dissolved lignin, and TLI is the total lignin content. EX is the content of acetone extractives. The determination accuracy of the lignin and the arabinose amounts was calculated to be 0.01%.

removed. One possibility to doing this is to apply a pulping process. There is a wide variety of different processes available and each has different effects and reaction mechanisms depending on the chemistry of the process.[18−24]

The aim of this work was to examine the tensile properties of kraft cooked Norway spruce using tensile testing and in situ X-ray diffraction. The macroscopic deformation of the samples and the deformation of crystalline cellulose in the samples were examined simultaneously, by monitoring the reflections *200* and *004* of cellulose as the samples were strained. The results were compared to similar studies on native Norway spruce, reported in a separate earlier publication.[25] The comparison made it possible to deduce the effect of the amorphous components on the tensile properties of crystalline cellulose in wood.

Materials and Methods

Samples. The sample material was Norway spruce (*Picea abies* [L.] Karst.), grown in Finland. The kraft cooks were made from wood chips, dried and screened according to the standard SCAN-CM 40:88. Pulping was performed in laboratory scale in a forced-circulation digester. The charge of active alkali was 21.5%, the liquid-to-wood ratio 4:1, and the sulfidity 30%. The initial temperature was 80 °C, and the heating-up rate was 1 °C /min. The final temperature was held at 170 °C for 150 min. Several batches of samples were collected, representing different stages of cooking. The samples used in the analysis were chosen from the stages where the final temperature was already reached (see Table 1). The pulped chips were carefully washed with tap water to maintain the original structure of wood. Yields and κ numbers were determined. κ numbers were determined according to standard SCAN-C 1:77.

The samples for the tensile tests were made from the kraft cooked wood chips by cutting with a scalpel. Only the earlywood region of a single annual ring was chosen for each sample. For more information on the structure of Norway spruce cells, see e.g. the review by Brändström.[26] The length of the samples varied between 14 and 23 mm, the width between 0.7 and 5 mm and the thickness between 0.3 and 1.0 mm. The area of the cross-section varied between 0.3 and 3.5 mm^2.

Tensile Testing and X-ray Diffraction Experiments. The tensile tests were performed with a computer-controlled stretching device that was designed and manufactured at the University of Kiel.[3,5] Strain was applied and monitored by a servo motor-controlled linear stage (Hauser EMD SMH82/Compax 1000SL/S2 motor/controller, SKF LTB110 linear stage). Force was measured by an Entran (ELPM-T1M-250N-/L3M) sensor with a maximum load of 250 N. In all tensile tests, the strain was applied vertically, along the direction of the wood cells.

For the experiments with in situ X-ray diffraction, the testing apparatus was set up at the beamline A2 of Hamburger Synchrotronstrahlungslabor (HASYLAB). The samples were stretched in wet condition with a speed of 0.2 or 2 μm per second. The span used in the tensile tests varied between 8 and 13 mm. The diffraction experiments were conducted in the perpendicular transmission geometry, where the incoming beam is perpendicular to the surface of the sample. The size of the synchrotron X-ray beam was 250 × 250 μm^2, controlled by the piezo-electrically driven microslits of the beamline. The wavelength of the radiation was 1.5 Å. Diffraction patterns were recorded by a 2D detector (Photonic Science Gemstar-2 HS, 92 mm × 69 mm area, pixel size 67 μm, 1200 × 1003 pixels). The time resolution of the individual diffraction patterns was 4 s (3 s exposure time, detector readout 1 s), but every other diffraction pattern was taken as a dark image, thus the total time resolution was 8 s. Combined to the straining speeds, this corresponded to a strain resolution of 1.6 or 16 μm per diffraction pattern. In one case (sample 7) the dark images were not recorded, and the strain resolution was 0.8 μm per diffraction pattern.

Tensile tests were performed without in situ X-ray diffraction at the University of Kiel using samples from the same material as tested at HASYLAB. The same testing apparatus as described above was used, the only modifications being a different force sensor (ENTRAN ELPM-T2M-125N-/L3M, maximum capacity 125 N) and a modified design of sample clamps with horizontal grooves to improve the efficiency of sample holding. The samples were stretched in dry condition with a speed of 0.8 or 1.6 μm per second. A span of 5 mm was used in all cases.

Chemical Analysis. After the measurements the chemical composition of the samples was analyzed.[27,28] The analysis included the carbohydrate content, the amount of lignin, and the amount of extractives. To analyze the carbohydrate content, the samples were air-dried and the dry mass of the samples was determined according to the standard SCAN-C 3:78. The air-dried samples (0.3 g) were first finely grounded (30 mesh). The hydrolysis was performed with 72% sulfuric acid (3 mL) in a water bath at 30 °C for 60 min. The hydrolyzate was diluted (∼84 mL) and placed into a sterilization autoclave at 120 °C for 60 min. After total hydrolysis the diluted (200 mL) solution was neutralized to pH 4 with anion-exchange resin. After neutralization the hydrolysis sample (50 mL), containing internal standard (rhamnose), was evaporated (∼2 mL) and reduction to corresponding alditols was effected with sodium borohydride (60 mg). Sodium ions were removed by a cation-exchange resin. The boric acid residues were removed as methyl esthers. Acetylation of alditols was performed under refluxing (120 °C) with acetic anhydride and pyridine (1:1). The samples were analyzed by gas−liquid chromatography using a capillary column NB-1701. The program was isothermic (210 °C). The temperature of the injector and detector was 260 °C. To analyze the extractives content, another part of the air-dried samples was finely ground (30 mesh) and then extracted by acetone with Soxhlet extraction apparatus. The extraction time was 6 h. Extractive content was determined from the weighted evaporated samples. The lignin content was determined according to the KCL standard 115b:82.

Data Analysis. From the stress−strain curves the tensile strength, the modulus of elasticity (MOE) and the elongation at fracture were analyzed. The tensile strength was found as the maximum stress of the samples at fracture (or at yield point), and the corresponding strain value gave the strain at fracture (or at yield). The MOE was analyzed by dividing the stress−strain curve into segments covering 0.2% of elongation. The MOE was determined as the slope of the first of these segments by a linear least-squares fit, taking into account the measure-

ment accuracy of stress. In two cases (samples 8 and 13) the second segment was used due to abnormalities in the beginning of the stress−strain curve.

The 2D diffraction patterns were transformed from rectangular (pixel) coordinates of the detector to polar coordinates (q, φ), where φ is the polar (or azimuth) angle and q is the magnitude of the scattering vector. Here q is given by

$$q = \frac{4\pi \sin(\theta)}{\lambda} \quad (1)$$

where θ is half of the scattering angle 2θ and λ is the wavelength. The structure of the cellulose unit cell, based on a recent report,[16] is shown in Figure 1. The intensity profiles of the reflections *200* and *004* of crystalline cellulose as a function of q were used to obtain information on the deformation of the unit cell. This was done by following the position q_{hkl} of the diffraction peak and the lattice spacing d_{hkl}, defined as

$$d_{hkl} = \frac{2\pi}{q_{hkl}} \quad (2)$$

as a function of strain. The dimensional change ϵ_{hkl} was calculated as

$$\epsilon_{hkl} = \frac{d_{hkl} - d_{hkl,0}}{d_{hkl,0}} \quad (3)$$

where d_{hkl} and $d_{hkl,0}$ refer to the lattice spacing of the reflection *hkl* in strained and initial state, respectively. ϵ_{hkl} for crystalline cellulose was calculated both in the direction of the cellulose chains and in perpendicular direction (Figure 1). This enabled the determination of the (X-ray) Poisson ratio of crystalline cellulose by

$$\nu = \nu_{ca} = -\frac{\epsilon_{200}}{\epsilon_{004}} \quad (4)$$

where ϵ_{004} is the strain in the direction of the cellulose chains and ϵ_{200} is the strain perpendicular to the chains. The Poisson ratio was determined from every measured diffraction pattern before and after yield/fracture and a weighted mean value was calculated.

The full width at half-maximum (fwhm) of the reflections *200* and *004* was also determined as a function of strain. This information was used to follow changes taking place in the cellulose crystallites. Based on the fwhm values prior to applied strain, the minimum initial width and length of the cellulose crystallites was calculated by the Scherrer formula

$$D_{hkl} = \frac{0.9\lambda}{\Delta_{hkl}\cos(\theta_{hkl})} \quad (5)$$

where D_{hkl} is the size calculated from the reflection *hkl*, λ is the wavelength, Δ_{hkl} is the fwhm of the reflection, and θ_{hkl} is half of the scattering angle. The calculated D_{hkl} are minimum values because the instrumental broadening of the diffraction peaks was not known.

The azimuthal intensity profile of the reflection *200* was used to determine the orientation distribution of cellulose microfibrils (microfibril angle, MFA) as a function of strain. The profiles were obtained by first summing the two symmetric halves of the entire intensity curve to reduce the angular range from 360° to 180°. The orientation of the intensity maximum of the profiles was then set to correspond to MFA 0°, i.e., to the orientation of the cell axis. Due to the observed asymmetry in the MFA distribution of single Norway spruce tracheid walls,[29] the MFA distribution was modeled as a sum of two Gaussian functions. To take into account double cell walls, the MFA model of two Gaussians was mirrored with respect to the orientation of the cell axis to obtain the model for the intensity profile. Since the utilized scattering geometry was perpendicular transmission, a narrow central Gaussian peak situated at the intensity maximum was also included in the fitting.[30] An additional Gaussian peak, corresponding to the high q tail of the clearly separate reflection *102* at around 55° azimuth from the cell axis, was also included in the profile. The fitting spanned from −90° to 90°, but only the two Gaussians whose allowable peak positions were from 0° to 45° were included in the MFA distribution. An example of the fitting is shown in Peura et al.[25] The areas of the fitted MFA distributions were normalized to unity, and the expectation value and the standard deviation of MFA were calculated from these distributions.

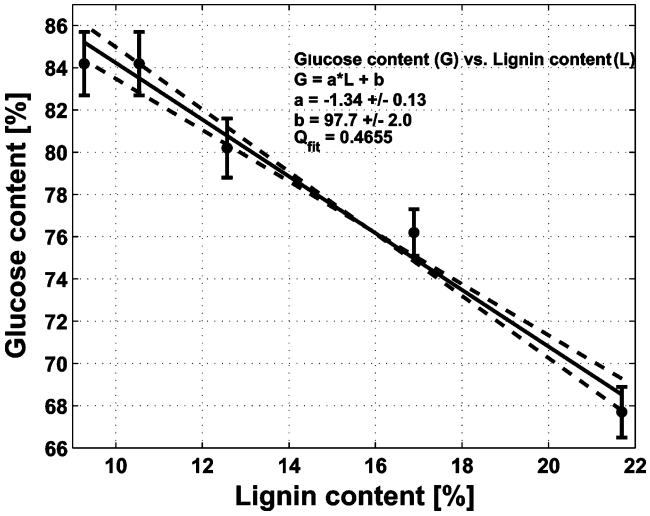

Figure 2. Glucose content of the samples as a function of the lignin content of the samples. The measurement accuracy of glucose content was taken into account in the fitting.

Table 2. Average Results of the Dry Samples, Grouped According to the Cooking Time[a]

t_C [min]	TS [MPa]	MOE [GPa]	ϵ_F [%]
120	41 ± 6	3.40 ± 0.43	3.6 ± 0.6
150	20 ± 3	2.04 ± 0.11	2.8 ± 0.4
180	47 ± 3	2.73 ± 0.31	4.8 ± 0.5
210	32 ± 10	2.32 ± 0.10	3.9 ± 0.5
240	72 ± 4	3.21 ± 0.19	5.1 ± 0.3

[a] t_C denotes the cooking time, TS is the tensile strength, MOE is the modulus of elasticity, and ϵ_F is the elongation at fracture.

Results

The chemical composition of the samples is presented in Table 1. As can be seen, the amount of lignin decreased from 21.7% to 9.3% as the cooking time increased from 120 to 240 min. The amount of hemicelluloses diminished relative to the amount of cellulose as the cooking time increased. The amount of extractives was on the same level, around 0.25% in all other samples except those which were cooked for 210 min, where the amount was 0.35%. The accuracy values were calculated using the law of error propagation. When the amounts of lignin and glucose were compared, a nearly linear relationship was found; see Figure 2.

Results of the tensile tests of dry samples are presented in Tables S1 and 2. Table S1 shows the results of individual samples (Supporting Information), whereas the results in Table 2 are weighted averages according to cooking time. The stress−strain curves are shown in Figure 3. The results of the tensile tests of wet samples with in situ X-ray diffraction are shown in Tables S2 and 3, and the stress−strain curves are shown in Figure 4. Table S2 shows the results of single samples (Supporting Information). The weighted averages according to the cooking time are presented in Table 3. The accuracy values

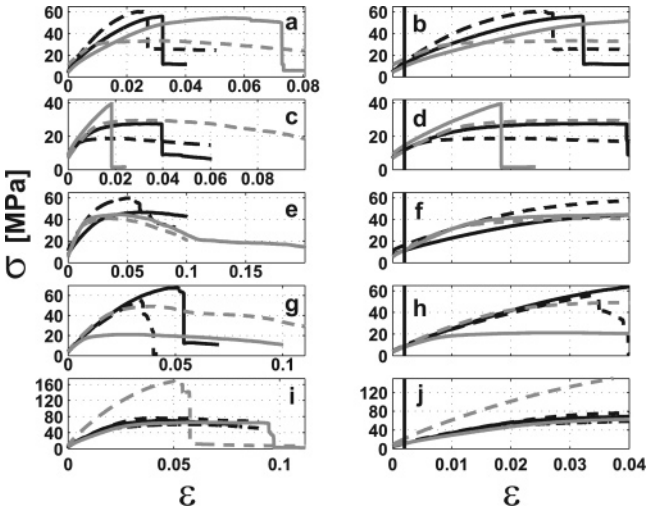

Figure 3. Stress−strain curves of the samples measured at the University of Kiel in dry condition. The figures on the left side show the entire stress−strain curves; on the right side, details from the first 4% of elongation are shown. In the detailed figures, vertical lines are drawn to show the range of MOE determination (from the start to 0.2% of elongation). The figures are arranged according to cooking time. a, b: 120 min (samples D1−D4); c, d: 150 min (samples D5−D8); e, f: 180 min (samples D9−D12); g, h: 210 min (samples D13−D16); i, j: 240 min (samples D17−D21). For more information on the samples, see Table S1.

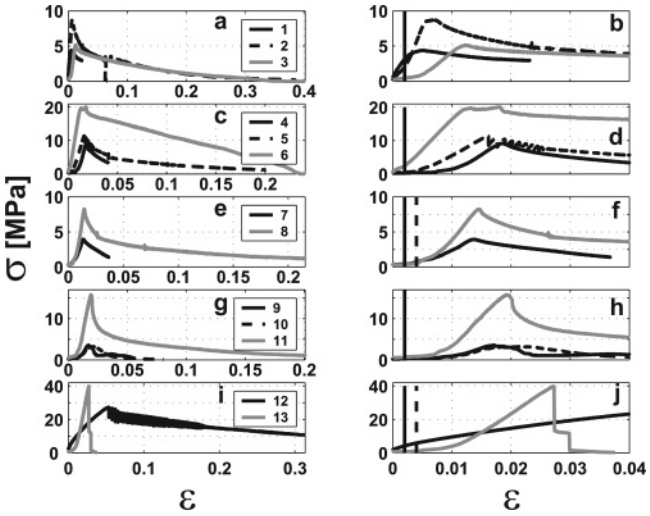

Figure 4. Stress−strain curves of the samples measured at HASYLAB in wet condition. The curves plotted with solid lines represent the samples selected for Figures 6, 7, and 9−12. The figure panes are arranged according to the cooking time. a, b: 120 min; c, d: 150 min; e, f: 180 min; g, h: 210 min; i, j: 240 min. In the figures showing the details (on the right side), vertical lines are drawn to show the range of MOE determination (from the start to 0.2% of elongation). In parts f and j a line is also drawn at 0.4% of elongation (MOE was determined from between 0.2% and 0.4% in samples 8 and 13).

presented in Tables S1 and S2 were calculated as weighted standard deviations of the measured quantities by using the law of error propagation. In Tables 2 and 3, the accuracy values were calculated as the weighted standard errors of the average values. The weights used in the calculations were the inverse square of the measurement accuracies of the individual measurements.

The tensile properties of both wet and dry kraft cooked samples exhibited large variations (Tables S1 and S2). On average, the samples cooked for the longest time had highest tensile strength in both wet and dry samples, 36 and 72 MPa, respectively. The average tensile strength of the samples from shorter cooking times was more uniform, and the values of wet samples were smaller than those of dry samples by a factor of 2−10. The elongation at fracture (or yield) was highest in the longest cooked samples in both dry and wet cases (Tables 2 and 3). In the case of wet samples, the elongation was smallest in the least cooked samples and, except for the samples cooked for 180 min, the elongation at yield increased when the cooking time was increased (Table 3). In the dry samples such a relation was not found (Table 2). The elongation at yield/fracture as a function of the mass fraction of lignin and glucose in wet and dry samples is shown in Figure 5. In wet samples, the samples with the highest glucose content and the lowest lignin content elongated the most. In dry samples the behavior was less clear. The average MOE was highest in the samples cooked the least amount of time in both wet and dry samples, 0.36 and 3.40 GPa, respectively (Tables 3 and 2). The average MOE of wet samples was considerably lower than that of dry samples by roughly between 1 and nearly 2 orders of magnitude.

The initial MFA distributions of some of the samples are shown in Figure 6. The number of samples presented in Figure 6 and in the subsequent figures was reduced to two samples per figure to improve clarity. The expectation values and the standard deviations of the initial MFA distributions ($\langle$MFA$\rangle$, σ_{MFA}) of the individual samples are presented in Table S2. The averages calculated according to cooking time are presented in Table 3. $\langle$MFA$\rangle$ was small, between 3° and 7° in all cases except sample 12, where it was 16° (Table S2). The standard deviation of the MFA distributions varied between 8° and 16°. The average values of $\langle$MFA$\rangle$ and σ_{MFA} are fairly constant among the different cooking times, except for the average $\langle$MFA$\rangle$ of the longest cooked samples (Table 3). This is due to the higher $\langle$MFA$\rangle$ of sample 12.

The change of $\langle$MFA$\rangle$ as a function of strain is shown in Figure 7. Most notable changes took place in samples 1, 3, and 12. The decline of $\langle$MFA$\rangle$ in sample 12 clearly followed the stress−strain curve; see Figure 4. In sample 3 $\langle$MFA$\rangle$ was also diminished in the very initial stage of straining, but there were large, seemingly random fluctuations in the values as well. In other samples, no systematic change toward smaller $\langle$MFA$\rangle$ was observed as a function of strain. Fluctuations were observed especially in the MFA range 15°−45°, but the changes were not linked to the stress−strain curves in any systematic way. Similar trends could also be observed with the σ_{MFA} as a function of strain. In sample 12, both $\langle$MFA$\rangle$ and σ_{MFA} diminished about 1°, whereas in sample 3 σ_{MFA} diminished about 7° and $\langle$MFA$\rangle$ about 3°. Examples of the fluctuations in the MFA distributions can be seen in Figure 8, where the MFA distributions of two samples (11 and 12) and the respective $\langle$MFA$\rangle$ values are presented as a function of strain.

The minimum initial width and length of the cellulose crystallites in the samples are presented in Table S2, the averages according to cooking time in Table 3. The width varied between (34.4 ± 0.8) Å and (42.3 ± 0.4) Å in the individual samples (Table S2). The average width was between 36.5 and 41.2 Å (Table 3). No clear correlation between cooking time and the average crystallite width could be observed. The length varied between (75.3 ± 0.4) Å and (165 ± 3) Å in the individual samples. The average length was between 77 and 144 Å. The samples cooked for the shortest amount of time exhibited longest crystallites, but the standard error of the average length was large in all cases. The smallness of the average length in the longest cooked samples is due to sample 12, which had considerably shorter crystallites than the other samples. The fwhm of the reflections *004* and *200* varied considerably in the

Table 3. Average Results of the Wet Samples, Grouped According to the Cooking Time[a]

t_C [mi n]	TS [MPa]	MOE [GPa]	ϵ_F [%]	ν_1	ν_2	⟨MFA⟩ [deg]	σ_{MFA} [deg]	D_{200} [Å]	D_{004} [Å]
120	5.1 ± 0.4	0.36 ± 0.33	0.82 ± 0.21	−1.06 ± 0.53	−0.98 ± 0.46	6 ± 1	12 ± 2	40.2 ± 1.0	144 ± 11
150	10.4 ± 1.2	0.12 ± 0.02	1.74 ± 0.10	−0.91 ± 0.25	−1.00 ± 0.19	5 ± 1	10 ± 1	41.2 ± 0.7	135 ± 10
180	5.5 ± 2.0	0.06 ± 0.03	1.42 ± 0.04	−0.76 ± 0.30	−0.86 ± 0.25	6 ± 1	10 ± 1	37.0 ± 0.7	125 ± 4
210	3.7 ± 1.4	0.03 ± 0.01	1.93 ± 0.13	−1.17 ± 0.26	−1.05 ± 0.26	5 ± 1	10 ± 1	40.8 ± 0.7	135 ± 6
240	36.3 ± 5.6	0.20 ± 0.16	4.0 ± 1.3	−0.26 ± 0.15	N/A	11 ± 6	12 ± 2	36.5 ± 1.4	77 ± 9

[a] t_C denotes the cooking time, TS is the tensile strength, MOE is the modulus of elasticity, and ϵ_F is the elongation at fracture. ν_1 is the average Poisson ratio of the cellulose unit cell, measured up to the yield point. ν_2 is the average Poisson ratio after the yield point. ⟨MFA⟩ and σ_{MFA} denote the expectation value and the standard deviation of the microfibril angle distribution prior to tensile tests. D_{200} and D_{004} are the minimum initial thickness and length of the cellulose crystallites, respectively.

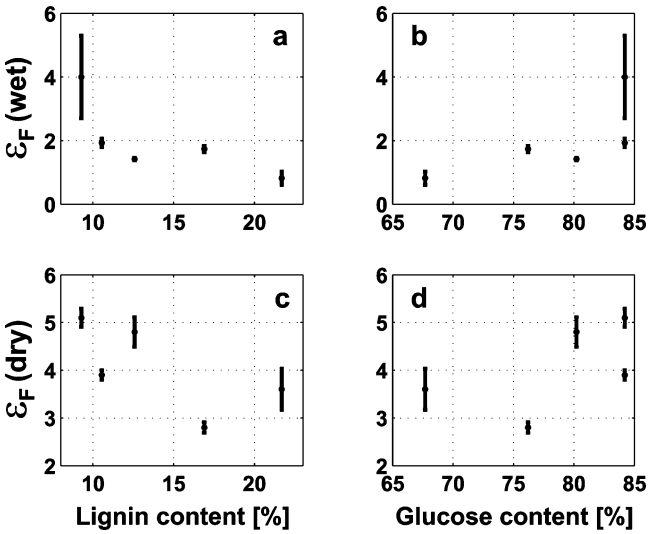

Figure 5. Elongation at fracture/yield in wet and dry samples as a function of lignin content (a, c) and glucose content (b, d).

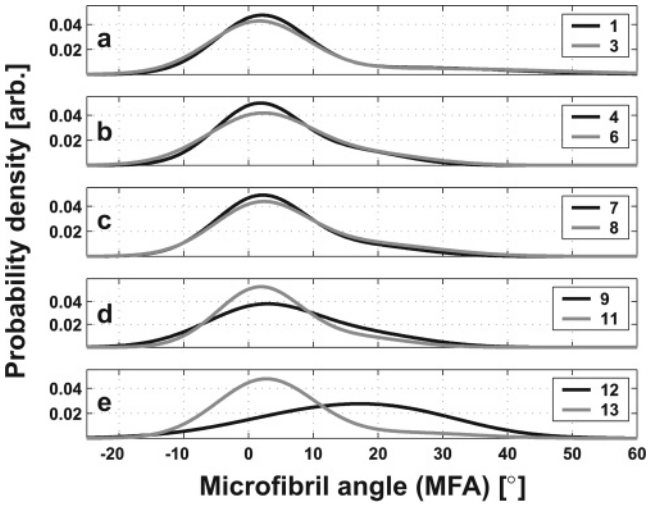

Figure 6. Microfibril angle distribution in selected wet samples prior to the tensile tests at HASYLAB. The distributions are arranged according to the cooking time. a: 120 min; b: 150 min; c: 180 min; d: 210 min; e: 240 min.

values, but only for sample 12 these variations could be linked to the stress−strain curve. In sample 12, the fwhm of *004* was slightly diminished by strain, but also in this case there were quite large fluctuations in the fwhm that were not due to the applied strain.

The strain in the direction of the cellulose chains, along the crystallographic *c* axis, is shown in Figure 9. Figure 10 shows the strain in perpendicular direction, along the axis *a*. In all cases except sample 1, there existed expansion of crystalline cellulose along both of the studied directions. In most cases the expansion continued beyond the yield point. In sample 13,

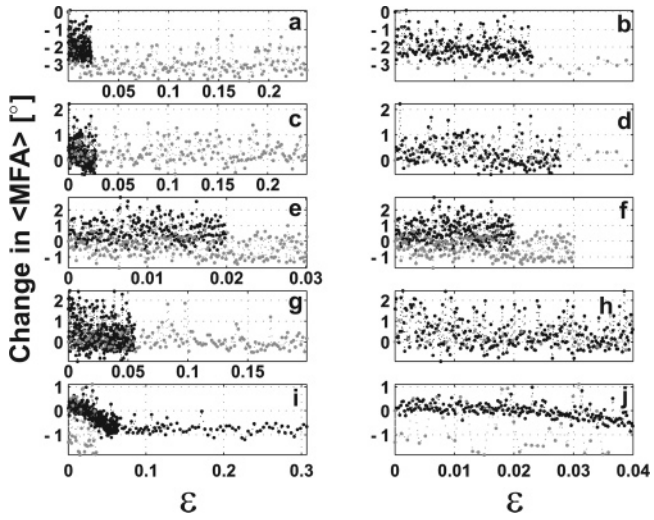

Figure 7. Change of the expectation value of MFA (⟨MFA⟩) as a function of strain. a, b: samples 1 (black) and 3 (gray), cooking time 120 min; c, d: samples 4 (black) and 6 (gray), cooking time 150 min; e, f: samples 7 (black) and 8 (gray), cooking time 180 min; g, h: samples 9 (black) and 11 (gray), cooking time 210 min; i, j: samples 12 (black) and 13 (gray), cooking time 240 min.

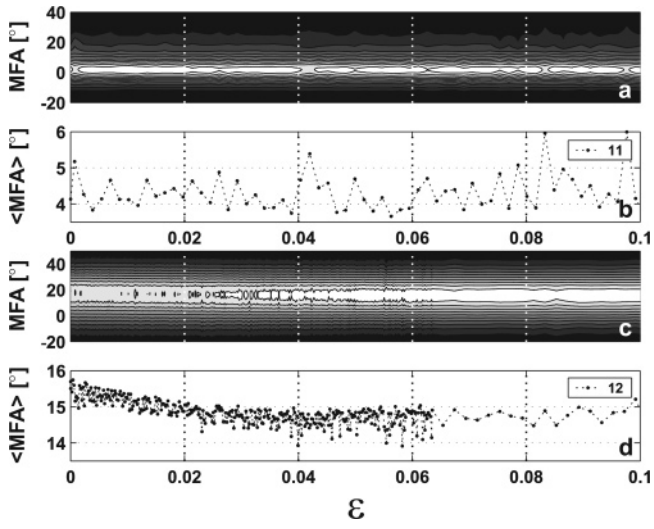

Figure 8. MFA distribution and the ⟨MFA⟩ as a function of strain in samples 11 and 12. a, b: sample 11; c, d: sample 12.

the dimensions of the unit cell returned to their initial values after the fracture of the sample, following the stress−strain curve closely especially in the direction along the cellulose chains. In other samples the stress−strain curves exhibited a more ductile behavior, also the strains of crystalline cellulose changed more gradually after the yield point.

The unit cell expanded both along the cellulose chains and in the perpendicular direction. This led to a negative (X-ray) Poisson ratio of crystalline cellulose in all cases. The obtained

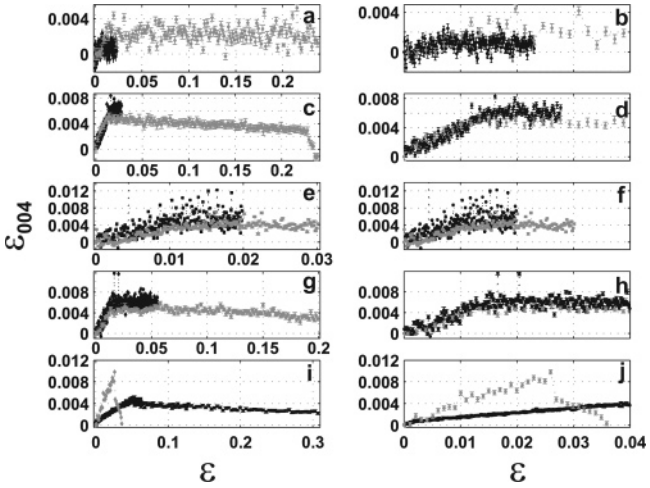

Figure 9. Strain of the cellulose unit cell along the crystallographic axis *c* as a function of strain. a, b: samples 1 (black) and 3 (gray), cooking time 120 min; c, d: samples 4 (black) and 6 (gray), cooking time 150 min; e, f: samples 7 (black) and 8 (gray), cooking time 180 min; g, h: samples 9 (black) and 11 (gray), cooking time 210 min; i, j: samples 12 (black) and 13 (gray), cooking time 240 min.

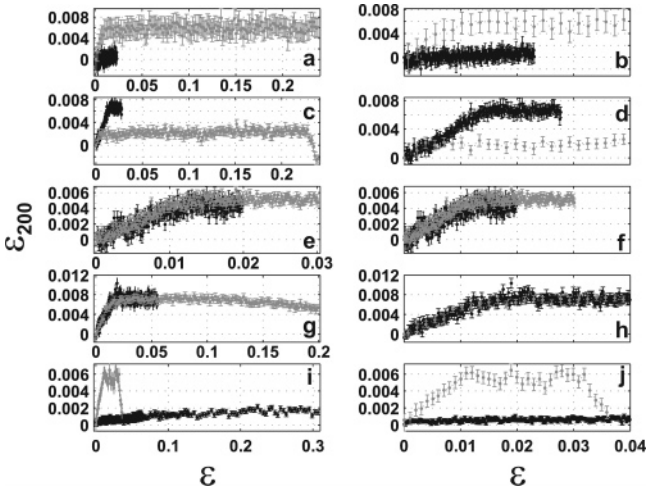

Figure 10. Strain of the cellulose unit cell along the crystallographic axis *a* as a function of strain. a, b: samples 1 (black) and 3 (gray), cooking time 120 min; c, d: samples 4 (black) and 6 (gray), cooking time 150 min; e, f: samples 7 (black) and 8 (gray), cooking time 180 min; g, h: samples 9 (black) and 11 (gray), cooking time 210 min; i, j: samples 12 (black) and 13 (gray), cooking time 240 min.

Poisson ratio was remarkably similar both before and after the yield point, although the Poisson ratios from the individual samples showed some variation (see Tables S2 and 3). No significant differences were found between the average Poisson ratios of the samples from 120 to 210 min of kraft cooking. The average values ranged between −0.76 and −1.17 before the yield point and between −0.86 and −1.05 after the yield point. The samples which were cooked for 240 min exhibited a significantly smaller average Poisson ratio (−0.26) than the other groups. This was mostly due to sample 12 which had significantly wider initial MFA distribution than the other samples and in which the MFA was also systematically affected by straining.

Discussion

Kraft cooking was used to remove lignin from the sample material. By using different cooking times a series of samples with different mass fractions of lignin was obtained. Also the proportion of hemicelluloses in the samples compared to cellulose was diminished as a function of cooking time, but the diminishing effect was smaller than that observed in the lignin content. The extractives content did not show significant changes due to the pulping process. When the mass fraction of lignin and glucose were compared, a negative correlation was found.

The initial MFA distributions were quite narrow in all samples, and the expectation value of MFA (⟨MFA⟩) was low in all samples except in sample 12. Therefore, the sample series had a fairly homogeneous microfibrillar arrangement. The small ⟨MFA⟩ is typical of normally grown Norway spruce wood from Finland.[31] The initial average crystallite thickness showed variation, but it was not directly connected to cooking time or to the content of lignin or glucose in the samples. The average initial thickness was larger and the average initial length was smaller than those reported for native Norway spruce earlywood.[25] The average initial length of the crystallites in kraft cooked samples was smaller than in untreated Norway spruce roughly by a factor of 2. The width was larger by 10−25% compared to untreated Norway spruce. Instrumental broadening (for comparison, 0.16° with the same setup at HASYLAB except for a different CCD detector) cannot give rise to such a substantial effect as observed in crystallite length between native and kraft cooked wood. The reflection *200* is in any case so wide that the small instrumental broadening does not have a significant effect on the calculated crystallite widths. A similar trend in both the length and the thickness of crystallites due to kraft cooking was observed in Scots pine samples, where the thickness of the cellulose crystallites increased from 30 to 34 Å and the length of the crystallites decreased to about half compared to the untreated samples.[32]

The tensile tests were all performed along the longitudinal direction of the cells. Since ⟨MFA⟩ was low, the applied strain was fairly parallel to the cellulose chains in the microfibrils. When the tensile strength and the MOE of wet and dry kraft cooked samples were compared, enormous differences were found. Both the tensile strength and the MOE were smaller in wet samples than in dry samples. The tensile stress was smaller roughly by a factor of 2−10, whereas the MOE was between 1 and 2 orders of magnitude smaller in wet than in dry samples. Also the elongation at yield/fracture was smaller in wet than in dry samples. In both wet and dry samples the longest cooked samples elongated the most; in wet samples the least cooked elongated the least. The tensile strength was highest in the longest cooked samples, followed by the least cooked samples. The MOE was highest in the least cooked samples, followed by the most cooked samples. This indicated that the material became more compliant as the cooking progressed, as was expected from the decreasing in the lignin content as the cooking time increased. The tensile strength and the MOE of the dry kraft cooked samples were fairly similar to those of native dry earlywood of Norway spruce tested with the same apparatus.[25] The differences in the tensile strength and the MOE between wet and dry kraft cooked samples were larger than the respective differences between a sample of native wet latewood (M. Peura et al., unpublished data) and similar dry samples.[25] These findings indicate that kraft cooking had a more noticeable effect on the tensile properties when the samples were tested in wet than in dry condition.

The orientation of cellulose microfibrils did not show systematic changes as a function of strain in most samples. In the sample set which was cooked the least, a reduction in ⟨MFA⟩ and σ_{MFA} took place in the very early stages of straining, but

thereafter the changes were fluctuations not connected to the stress−strain curves. In sample 12, ⟨MFA⟩ and σ_{MFA} decreased as a function of strain before the yield point. After the yield point, ⟨MFA⟩ and σ_{MFA} were more or less constant. A similar reduction has been observed in wet Norway spruce with high ⟨MFA⟩.[2] The result that MFA did not change much as a function of strain when the distribution was initially narrow and the expectation value was small was similar to untreated dry Norway spruce.[25]

The fwhm of the reflection *200* did not show marked changes due to straining. The fwhm of *004* exhibited similar behavior in all samples but sample 12, in which the fwhm diminished. In that sample also the MFA was affected. This is contrary to untreated Norway spruce,[25] where clear diminishing effects were observed in the fwhm of *004* as the samples were stretched, even while the MFA was not affected. In that study the fwhm of *200* did not show changes as a function of strain, similar to results presented here.

Stretching the samples had a clear effect on crystalline cellulose. The cellulose chains in the crystallites elongated on the basis of the shift of the reflection *004*. The shift of the reflection *200* indicated that the distance of the hydrogen bonded sheets in the crystallites increased. This is contrary to untreated dry Norway spruce.[25] In crystallites of the untreated samples the length of the chains increased and the distance of the sheets contracted. The tensile behavior where expansion occurs both along the strain and in perpendicular direction leads to a conclusion that crystalline cellulose in kraft cooked Norway spruce is an *auxetic* material, i.e., it exhibits a negative Poisson ratio.

In a pioneering study,[33] it was calculated that auxeticity could be found in the in-plane direction of paper. The calculated magnitude of the Poisson ratio was smaller than −0.10. In this report the microstructure of wood cells was not taken into account. Auxeticity has been observed in an out-of-plane direction of paper.[34] In the hardwoods basswood, cottonwood, and soft maple, negative Poisson ratios between −0.036 and −0.316 were observed when the samples were stretched nonparallel to the orientation of the cells, at an angle of 20° to the longitudinal−tangential plane.[35] From other biological material, the auxeticity of skin tissue has been discussed.[36] However, in these studies the results were obtained from macroscopical samples.

Overall, there have been many reports on auxetic materials. Most of these represent human-made materials, such as foams,[37] polymer chains,[38] or expanded polymer networks.[39] Auxeticity has also been reported on crystalline materials with a monoclinic crystal structure,[40] which is also the structure of crystalline cellulose I_β.[13] There are also reports on theoretical calculations and simulations which produce negative Poisson ratios for a variety of different systems. These include isotropic materials,[41] single crystals,[42] honeycomb structures,[43] fibrillar networks,[44−46] composite structures,[47] and even extreme states of matter.[48] To the authors' knowledge, the results presented here are the first report of a biopolymer with measured auxetic tensile behavior in the crystalline regions.

It has been discussed that, perpendicular to the longitudinal cell axis, the amorphous lignin−hemicellulose matrix has a definite role for the mechanical properties of wood cells.[17] This was shown to be true between early- and latewood and juvenile and mature wood of Norway spruce; the different types of wood exhibited different Poisson ratios of crystalline cellulose.[25] In that study, however, all of the Poisson ratios were of positive sign, the averages ranging between 0.28 ± 0.10 and 0.82 ± 0.11. For ramie cellulose, values of 0.54 ± 0.09 and 0.38 ± 0.04 have been reported.[3,49] For flax cellulose, a value of 0.46 ± 0.10 has been obtained.[3] The negative Poisson ratios for kraft cooked samples indicate that when the lignin−hemicellulose matrix is removed, the mechanical properties of crystalline cellulose are dramatically altered. Moisture is not responsible for the effect; also wet untreated wood exhibited a positive Poisson ratio (M. Peura et al., unpublished).

Crystalline cellulose is most susceptible to changes in the environment around it along the axis *a*. The expansion observed in this direction due to strain is caused by the microfibrillar arrangement of the wood cells. The cellulose microfibrils are seldom oriented strictly parallel to the applied strain in the sample. Nearly always there exists a component of the straining force that acts perpendicular to the hydrogen-bonded sheets. In normally grown wood, the amorphous matrix of lignin and hemicelluloses provides support to crystalline cellulose along the axis *a*, and the Poisson ratio is positive. When wood is pulped, in this case by kraft cooking, the lignin−hemicellulose matrix is gradually removed, starting from the lumina of the wood cells and proceeding toward the middle lamella without a significant lignin gradient in the secondary cell wall.[21,50−52] Only after the samples have been delignified by more than 50% is the middle lamella significantly and quite rapidly affected. The order of progression of the delignification explains why the observed Poisson ratio was negative already in the samples cooked for the least amount of time.

The removal of lignin and hemicelluloses causes the formation of pores in the cell wall structure[19,53−55] and an increase in the degree of order in cellulose.[56,57] It also leads to the swelling of the cellulose crystallites in the crystallographic *a* direction.[18,32,58] When the cooking process is taken to low κ numbers, there exists some aggregation of cellulose microfibrils as the result of low residual hemicellulose content.[59,60] Moreover, the residual lignin is mostly chemically bound to different hemicelluloses, not to cellulose, and the bonding of the residual lignin to specific hemicelluloses varies as the κ number of the pulp is altered.[61, 62]

In kraft cooked wood the crystalline cellulose still retains the helical arrangement around the lumina of the cells, even though the amorphous matrix is altered or removed. Since crystalline cellulose is not well bound to the reduced amorphous matrix of the cell wall, the component of the straining force perpendicular to the hydrogen-bonded sheets can cause the expansion also in that direction. In the samples cooked to lower κ numbers, the expansion can also be partly due to shearing interactions between individual cells and cell wall layers with different microfibril orientations. In the samples with low κ numbers, the cells are no longer held together rigidly by the middle lamellae but can slide past one another. This effect should be more prominent around and after the yield point in the stress−strain curve.

Conclusions

The tensile properties of earlywood samples of kraft cooked Norway spruce were studied. Prior to the applied strain, the cellulose crystallites were shorter and wider in kraft cooked samples compared to native Norway spruce wood, while the MFA distribution was narrow also in kraft cooked samples. The tensile properties of dry kraft cooked samples were fairly similar to those of native Norway spruce earlywood. The tensile properties of wet kraft cooked samples differed dramatically from the dry samples. The microfibril angle distribution was

not much affected by straining, except in the case where the initial expectation value of MFA was fairly large. There a systematic diminishing effect was noted before the yield point in the stress−strain curve. Crystalline cellulose in kraft cooked Norway spruce was shown to have a negative Poisson ratio, i.e., it exhibited auxetic tensile behavior. Expansion took place both along the cellulose chains and in the direction perpendicular to the hydrogen-bonded sheets of cellulose chains. On the basis of the structure of crystalline cellulose and on the structure of wood cells, possibilities contributing to the auxeticity were discussed. These included the effect of the microfibrillar orientation and the shearing interactions between neighboring cells and cell wall layers.

Acknowledgment. The authors are grateful to Timo Pääkkönen of the Helsinki University of Technology, Laboratory of Forest Products Chemistry, for making the kraft cooked samples. The authors thank Dr. Sergio Funari and M.Sc. Martin Dommach of HASYLAB, for their assistance during the measurements at beamline A2. The Academy of Finland is gratefully acknowledged for financing (Grant 104837). The Finnish Academy of Science and Letters is gratefully acknowledged for providing funding for the measurement journeys.

Supporting Information Available. Tables S1 and S2, which show the results from the individual samples, are given as Supporting Information. This material is available free of charge at http://pubs.acs.org.

References and Notes

(1) Wagenführ, R.; Scheiber, I. C. *Holzatlas*, *3. Auflage*; Leipzig: Fachbuchverlag VEB, 1989.
(2) Keckes, J.; Burgert, I.; Frühmann, K.; Müller, M.; Kölln, K.; Hamilton, M.; Burghammer, M.; Roth, S. V.; Stanzl-Tschegg, S.; Fratzl, P. *Nat. Mater.* **2003**, *2*, 810−814.
(3) Kölln, K. Ph.D. Thesis. University of Kiel, 2004. Available online at http://e-diss.uni-kiel.de/diss_1173.
(4) Kamiyama, T.; Suzuki, H.; Sugiyama, J. *J. Struct. Biol.* **2005**, *151*, 1−11.
(5) Kölln, K.; Grotkopp, I.; Burghammer, M.; Roth, S. V.; Funari, S. S.; Dommach, M.; Müller, M. *J. Synchrotron Rad.* **2005**, *12*, 739−744.
(6) Mott, L.; Shaler, M.; Groom, L. H. *Wood Fiber Sci.* **1996**, *28*, 429−437.
(7) Sippola, M.; Frühmann, K. *Holzforschung* **2002**, *56*, 669−675.
(8) French, J.; Conn, A. B.; Batchelor, W. J.; Parker, I. H. *Appita J.* **2000**, *53*, 210−226.
(9) Sinn, G.; Reiterer, A.; Stanzl-Tschegg, S. E.; Tschegg, E. K. *Holz Roh- Werkst.* **2001**, *59*, 177−182.
(10) Åkerholm, M.; Salmén, L. *Polymer* **2001**, *42*, 963−969.
(11) Åkerholm, M.; Salmén, L. *Holzforschung* **2003**, *57*, 459−465.
(12) Eichhorn, S. J.; Sirichaisit, J.; Young, R. J. *J. Mater. Sci.* **2001**, *36*, 3129−3135.
(13) Gardner, K. H.; Blackwell, J. *Biopolymers* **1974**, *13*, 1975−2001.
(14) Woodcock, C.; Sarko, A. *Macromolecules* **1980**, *13*, 1183−1187.
(15) Tashiro, K.; Kobayashi, M. *Polymer* **1991**, *32*, 1516−1526.
(16) Nishiyama, Y.; Langan, P.; Chanzy, H. *J. Am. Chem. Soc.* **2002**, *124*, 9074−9082.
(17) Salmén, L. *C. R. Biologies* **2004**, *327*, 873−880..
(18) Parks, L. R. *Tappi* **1959**, *42*, 317−319.
(19) Stone, J. E.; Scallan, A. M. *Pulp. Pap. Mag. Can.* **1968**, *69*, T288−T293.
(20) Kettunen, J.; Laine, J. E.; Yrjala, I.; Virkola, N. E. *Pap. Ja Puu-Pap. Timber* **1982**, *64*, 205−211.
(21) Saka, S.; Thomas, R. J. *Wood Fiber* **1982**, *14*, 144−158.
(22) Atalla, R. H.; Ranua, J.; Malcolm, E. W. *Tappi J.* **1984**, *67*, 96−99.
(23) Young, R. A. *Cellulose* **1994**, *1*, 107−130.
(24) Hult, E. L.; Larsson, P. T.; Iversen, T. *Holzforschung* **2002**, *56*, 179−184.
(25) Peura, M.; Kölln, K.; Grotkopp, I.; Saranpää, P.; Müller, M.; Serimaa, R. Submitted for publication.
(26) Brändström, J. *IAWA J.* **2001**, *22*, 333−353.
(27) Sjöström, E.; Haglund, P.; Janson, J. *Svensk Papperst.* **1966**, *69*, 381−385.
(28) Janson, J. *Pap. Ja Puu-Pap. Timber* **1970**, *52*, 323−329.
(29) Peura, M.; Müller, M.; Serimaa, R.; Vainio, U.; Sarén, M.-P.; Saranpää, P.; Burghammer, M. *Nucl. Inst. Methods B* **2005**, *238*, 16−20.
(30) Sarén, M.-P.; Serimaa, R.; Andersson, S.; Saranpää, P.; Keckes, J.; Fratzl, P. *Trees* **2004**, *18*, 354−362.
(31) Sarén, M.-P.; Serimaa, R.; Andersson, S.; Paakkari, T.; Saranpää, P.; Pesonen, E. *J. Struct. Biol.* **2001**, *136*, 101−109.
(32) Hattula, T. *Pap. Ja Puu-Pap. Timber* **1986**, *12*, 926−931.
(33) Cox, E. L. *Br. J. Appl. Phys.* **1952**, *3*, 72−79.
(34) Stenberg, N.; Fellers, C. *Nordic Pulp Pap. Res. J.* **2002**, *17*, 387−394.
(35) Sliker, A.; Yu, Y. *Wood Fiber Sci.* **1993**, *25*, 8−22.
(36) Veronda, D. R.; Westmann, R. A. *J. Biomech.* **1970**, *3*, 111−122.
(37) Lakes, R. *Science* **1987**, *235*, 1038−1040.
(38) He, C.; Liu, P.; Griffin, A. C. *Macromolecules* **1998**, *31*, 3145−3147.
(39) Caddock, B. D.; Evans, K. E. *Biomaterials* **1995**, *16*, 1109−1115.
(40) Rovati, M. *Scripta Mater.* **2004**, *51*, 1087−1091.
(41) Rothenburg, L.; Berlin, A. A.; Bathurst, R. J. *Nature* **1991**, *354*, 470−472.
(42) Milstein, F.; Huang, K. *Phys. Rev. B* **1979**, *19*, 2030−2033.
(43) Masters, I. G.; Evans, K. E. *Composite Struct.* **1996**, *35*, 403−422.
(44) Boal, D. H.; Seifert, U.; Shillcock, J. C. *Phys. Rev. E* **1993**, *48*, 4274−4283.
(45) Pikhitsa, P. V. *Phys. Rev. Lett.* **2004**, *93*, 015505−1−015505−4.
(46) Delannay, F. *Int. J. Sol. Struct.* **2005**, *42*, 2265−2285.
(47) Wei, G.; Edwards, S. F. *Physica A* **1998**, *258*, 5−10.
(48) Baughman, R. H.; Dantas, S. O.; Stafström, S.; Zakhidov, A. A.; Mitchell, T. B.; Dubin, D. H. E. *Science* **2000**, *288*, 2018−2022.
(49) Nakamura, K.; Wada, M.; Kuga, S.; Okano T. *J. Polym. Sci. B* **2004**, *42*, 1206−1211.
(50) Wardrop, A. B. *Svensk Papperst.* **1963**, *66*, 231−247.
(51) Procter, A. R.; Yean, W. Q.; Goring, D. A. I. *Pulp Pap. Mag. Can.* **1967**, *10*, T445−T453, T460.
(52) Wood, J. R.; Goring, D. A. I. *Pulp Pap. Mag. Can.* **1973**, *74*, T309−T313.
(53) Andreasson, B.; Forsström, J.; Wågberg, L. *Cellulose* **2003**, *10*, 111−123.
(54) Laine, C.; Wang, X.; Tenkanen, M.; Varhimo, A. *Holzforschung* **2004**, *58*, 233−240.
(55) Fahlén, J.; Salmén, L. *Biomacromolecules* **2005**, *6*, 433−438.
(56) Evans, R. E.; Newman, R. H.; Roick, U. C.; Suckling, I. D.; Wallis, A. F. A. *Holzforschung* **1995**, *49*, 498−504.
(57) Hult, E. L.; Larsson, P. T.; Iversen, T. *Cellulose* **2000**, *7*, 35−55.
(58) Hult, E. L.; Iversen, T.; Sugiyama, J. *Cellulose* **2003**, *10*, 103−110.
(59) Duchesne, I.; Hult, E. L.; Molin, U.; Daniel, G.; Iversen, T.; Lennholm, H. *Cellulose* **2001**, *8*, 103−111.
(60) Duchesne, I.; Takabe, K.; Daniel, G. *Holzforschung* **2003**, *57*, 62−68.
(61) Lawoko, M.; Henriksson, G.; Gellerstedt, G. *Holzforschung* **2003**, *57*, 69−74.
(62) Lawoko, M.; Berggren, R.; Berthold, F.; Henriksson, G.; Gellerstedt, G. *Holzforschung* **2004**, *58*, 603−610.

BM050722O